Full text open access online (Since 2001)

PRINT: ISSN 0972-3757 ONLINE: ISSN 2456-6330
Int J Hum Genet, 23(1): 34-41 (2023)
DOI: 10.31901/24566322.2023/23.01.802

Therapeutic Effects of Baicalin on Degeneration of Intervertebral Disk Cartilage Endplate Cells by Inhibiting IL-1β Activation via the NF-κB Pathway

Yukun Zhang[1], Huihua Zhai[2], Jun Ren[3] and Weibin Sheng[1,*]

[1]Department of Spine Surgery, The First Affiliated Hospital of Xinjiang Medical University, Urumqi 830054, Xinjiang Uygur Autonomous Region, China
[2]Department of Anesthesia, Xinjiang Production and Construction Corps Hospital, Urumqi 830002, Xinjiang Uygur Autonomous Region, China
[3]Department of Spine Surgery, The Six Affiliated Hospital of Xinjiang Medical University, Urumqi 830002, Xinjiang Uygur Autonomous Region, China

KEYWORDS Baicalin. Cartilage Endplate Cells. Degeneration. Interleukin-1β. Intervertebral Disk. Nuclear Factor-κB

ABSTRACT We aimed at the assessment of efficacy of baicalin (BAI) on the degeneration of intervertebral disc (IVD) cartilage endplate-derived stem cells (CESCs). CESCs fell into control, IL-1β and BAI groups. MTT assay and EdU staining were employed for proliferation examination, and Annexin V-FITC/PI staining for apoptosis monitoring. The mRNA expressions of IL-6, aggrecan (Acan) and type II and X collagens were measured using RT-qPCR, and the protein expressions of type II collagen, Acan and matrix metalloproteinase (MMP)-3 were measured using immunofluorescence (IF) staining. Compared with IL-1β group, 12.5, 25 and 50 μg·mL-1 BAI groups had weakened apoptosis ability, decreased mRNA levels of IL-6 and type X collagen, reduced protein levels of NF-κB p65, MMP-1, MMP-3 and MMP-13, and increased mRNA levels of type II collagen and Acan in dose-dependent manners ($P<0.05$). Through regulating the NF-κB pathway, BAI inhibits the apoptosis of CESCs and the degradation of extracellular matrix induced by IL-1β, and reduces the cellular inflammatory level, thereby alleviating degradation.

INTRODUCTION

Intervertebral disc degeneration (IVDD) is the main attributor to lower back pain (Yang et al. 2020). Since there are no blood vessels in the IVD, nutrition supply and material metabolism are realized primarily by the cartilage endplate (CEP) (Cazzanelli et al. 2020). In the case of endplate damage, inflammatory cell infiltration, IVD fibrosis and reduction of extracellular matrix (ECM) occur, and IVD undergoes progressive structural changes, ultimately resulting in function loss and lower back pain (Luo et al. 2021). IVDD has a complicated molecular mechanism (Wang et al. 2019). Inflammatory mediators such as interleukin-1β (IL-1β) and matrix metalloproteinases (MMPs), as well as cytokines are highly active in degenerated IVD (Zhang et al. 2021). IL-1β is crucial for the degeneration of IVD chondrocytes, which mainly stimulates CEP-derived stem cells (CESCs) to produce MMPs, breaks down collagen fibers and destroys ECM, thus accelerating CEP degradation (Liu et al. 2021).

[*]Address for correspondence:
Weibin Sheng
E-mail: shengwbfahxmu@xamy-edu.cn

Baicalin (BAI), as an extract from the roots of Scutellaria baicalensis, can resist inflammation, oxidation, aging, cancer and virus (Huang et al. 2019). As an ideal anti-inflammatory drug, BAI has been widely applied to alleviate systemic and local inflammation in clinical practice, such as pneumonia (Zhang et al. 2021), osteoarthritis (Wang et al. 2021), neuroinflammation (Li et al. 2020) and allergic rhinitis (Li et al. 2020). However, whether BAI can suppress the effect of IL-1β on CESCs has not been reported yet.

Objectives

Therefore, this study aimed at the assessment of the of BAI on the degeneration of IVD CESCs.

MATERIAL AND METHODS

Materials, Reagents and Apparatus

The materials, reagents and apparatus used herein included rat CESCs and cell culture medium [Wuhan Procell Life Science & Technology Co., Ltd. (China]], BAI [Beijing Solarbio Science

& Technology Co., Ltd. (China]], recombinant human IL-1β protein [Beijing T&L Biotechnology Co., Ltd. (China]], methyl thiazolyl tetrazolium (MTT) assay kit [Shanghai Zeye Biotechnology Co., Ltd. (China]], apoptosis assay kit [Beijing BioLab Biotechnology Co., Ltd. (China]], primers of IL-6, Acan and type II and type X collagens [Suzhou GENEWIZ Biotechnology Co., Ltd. (China)], Antibodies against NF-κB p65, MMP-1, MMP-3, MMP-13, Acan and type II collagen II [CST (USA)], horseradish peroxidase-labeled secondary antibodies [Beijing Bersee Science and Technology Co., Ltd. (China)], TRIzol reagent, SYBR Green, glyceraldehyde-3-phosphate dehydrogenase (GAPDH), a microplate reader and bicinchoninic acid (BCA) assay kit [Thermo Fisher Scientific (USA)], A refrigerated centrifuge [Beckman (USA)], Image-Pro Plus 6.0 software (Media Cybernetics, USA) and protein electrophoresis system, membrane transfer apparatus and gel imager [Bio-Rad (USA)].

Cell Culture

The rat CESCs were collected by centrifugation, and routinely cultured with complete medium containing 10 percent fetal bovine serum under the conditions of 37°C and 5 percent CO_2. The medium was refreshed every 2 d. When the density reached 80 percent, the CESCs underwent digestion by 0.25 percent trypsin and passaged.

Detection of Viability of CESCs

P2-generation rat CESCs were inoculated into a 96-well plate (2×10^3/well), and underwent 24-h stimulation by BAI at 0, 12.5, 25, 50, 75 and 100 ìg·mL-1 and 4-h incubation with MTT at 37°C. After centrifugation and the removal of the supernatant, dimethyl sulfoxide (DMSO) was added. The microplate reader was employed to take measurement of the optical density at 450 nm (OD450). The BAI concentration corresponding to the cell viability rate of >80 percent was determined as the non-cytotoxic concentration for later experiments.

Detection of Cell Proliferation by MTT Assay and 5-ethynyl-2'-deoxyuridine (EdU) Staining

MTT assay: P2-generation rat CESCs were inoculated into a 96-well plate (5×10^3/well), and divided into control group (routinely cultured), IL-1β group (10 ng·mL-1 IL-1β was added into complete medium) and BAI group. Then the BAI group was further divided into 12.5, 25 and 50 μg·mL-1 BAI groups (12.5, 25 or 50 μg·mL-1 BAI was added into complete medium containing 10 ng·Ml-1 IL-1β). After 24-, 48-, 72- and 96-h culture, the CESCs received 4-h incubation with MTT at 37°C. Subsequent to centrifugation and the removal of the supernatant, DMSO was added, and an estimate of OD450 was conducted by use of the microplate reader.

EdU staining: At the density of 3×10^5/well, 24-h CESC culture was carried out subsequent to inoculation into a 24-well plate, followed by staining according to the instructions of EdU staining kit, fixation and mounting. Finally, statistical analysis was implemented with the aid of LAS-AF-Lite software (Leica Microsystems CMS GmbH, Germany).

Detection of CESC Apoptosis through Annexin V-FITC/PI Staining

The CESCs were inoculated into a 6-well plate, cultured for 48 h, digested with trypsin, and collected by centrifugation. Then they were suspended with 500 mL of binding buffer and underwent 15-min staining by Annexin V-FITC/PI (5 mL each) at room temperature in dark. At last, flow cytometry was conducted.

Detection of mRNA Expressions of IL-6, Acan and type II and X Collagen by Reverse Transcription-quantitative Polymerase Chain Reaction (RT-qPCR)

The total RNA from CESCs was achieved with the aid of by TRIzol reagent, and reversely transcribed into cDNA using RT kit, followed by amplification by SYBR Green, with GAPDH as an internal reference. PCR was implemented under the following conditions: pre-denaturation at 95°C for 30 s and 40 cycles × (95°C for 10 s and 60°C for 30 s). $2^{-\Delta\Delta CT}$ was employed to achieve a calculation of the relative mRNA expression levels of IL-6, Acan and type II and X collagens. The PCR primer sequences were as follows: IL-6: F: 5'-TGTTTCCCCTCATCTTTCC-3', R: 5'-GTGG-TATCTGTGCTTCTCTCC-3'. Type II collagen: F: 5'-GAGAATGGCGACTACAATC-3', R: 5'-GAA-

CAGCAGGTGCTAAACTG-3'. Type X collagen: F: 5'-GATTAGCACCTGCTAAACTG-3', R: 5'-GAACAGCAAGTGCTAAACTG-3'. Acan: F: 5'-TGATGCTGTATTGGCTGCACC-3', R: 5'-CTACATGGTTGTCAGGAATGTGT-3'. GAPDH: F: 5'-GGTGAAGGTCGGAGTGAACG-3', R: 5'-CGTGGGTGGAATCATACTGGA-3'.

Detection of Protein Expressions of Type II Collagen, Acan and MMP-3 by Immunofluorescence (IF) Staining

After the density was adjusted to 4×10^4/well, the CESCs were inoculated into a 24-well plate, fixed with 4 percent paraformaldehyde for 15-20 min, washed by PBS containing 0.1 percent Tween-20, incubated with 0.2 percent TritonX-100 for 15 min, and mounted with 5 percent serum for 1 h, followed by incubation with primarily antibodies targeting type II collagen (dilution ratio = 1: 100), Acan (dilution ratio = 1: 50) and MMP-3 (dilution ratio = 1: 100) primary antibodies at 4°C overnight. Then the CESCs received 1-h incubation with FITC-conjugated secondary antibodies at 37°C, followed by nuclear staining with DAPI, mounting and observation under a fluorescence microscope (200×; Olympus, Japan). Finally, Image-Pro Plus 6.0 software was utilized for the quantification of the fluorescence intensity.

Detection of NF-κB p65, MMP-1 and MMP-13 Expressions by Western Blotting (WB)

Subsequent to lysis using lysis buffer and centrifugation of the CESCs, the resulting supernatant was the protein sample, and the measurement of its concentration was implemented with the aid of the BCA protein assay kit. After quantification and denaturation, SDS-PAGE was employed for protein sequestration, along with a quick protein transfer onto a PVDF membrane. After 2-h blocking with TBST solution comprising 5 percent skim milk at room temperature, the membrane received incubation with primary antibodies targeting NF-κB p65, MMP-1 and MMP-13 (dilution ratio: 1: 2,000) at 4°C throughout the night. Subsequent to rinsing by TBST 3 times, secondary antibodies (dilution ratio = 1: 10,000) were added for protein incubation at room temperature for 2 h. At length, the color was developed with ECL developer, and the protein gray level was recorded by the Bio-Rad gel imager and photographed. With GAPDH as the control, relative quantitative analysis was performed.

Statistical Analysis

SPSS22.0 software (IBM, USA) was used for statistical processing. Measurement data were described as ($\bar{x} \pm s$), and detected by the independent *t* test. The significance level was set at $P<0.05$.

RESULTS

Effect of BAI on CESC Viability

The MTT assay results showed that 50 μg·mL^{-1} BAI was not instrumental to dramatically inhibiting the CESC viability ($P>0.05$). When the concentration of BAI reached 75 μg·mL^{-1}, the CESC viability could be significantly inhibited ($P<0.05$), suggesting that high-dose BAI had a certain toxic effect on CESCs (Fig. 1). Therefore, 50 μg·mL^{-1} was selected as the highest concentration to ensure the least effect of CESC on cell viability.

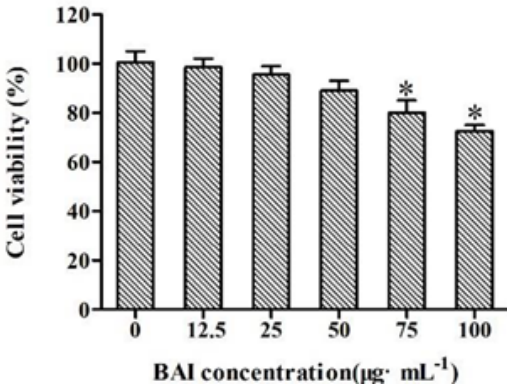

Fig. 1. Effect of BAI on viability of CESCs. *P<0.05 *vs.* control group. BAI: Baicalin.

CESC Proliferation Ability

As unveiled by the results of MTT assay, IL-β had strikingly abated OD values than control group ($P<0.05$) but dramatically elevated values than 12.5, 25 and 50 μg·mL^{-1} BAI groups at 24, 48, 72 and 96 h ($P<0.05$) (Fig. 2). It was found by EdU staining that the proportion of EdU-positive cells

was pronouncedly lower in IL-1β group than that in control group (P<0.05), while it was noticeably higher in 12.5, 25 and 50 μg·mL^{-1} BAI groups than that in IL-1β group (P<0.05) (Fig. 3). Collectively, BAI restored the proliferation ability of cells damaged by IL-1β in a dose-dependent manner.

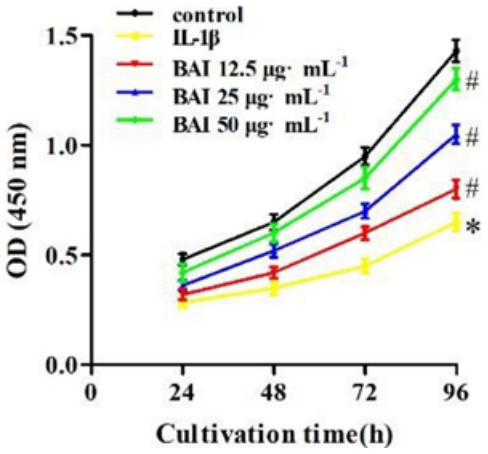

Fig. 2. Cell survival ability. *P<0.05 *vs*. control group, #P<0.05 *vs*. IL-1β group. IL-1β: Interleukin-1β.

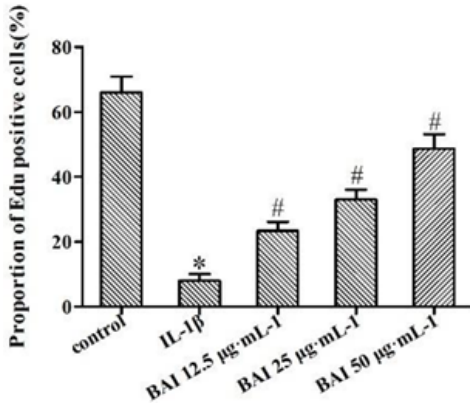

Fig. 3. Cell proliferation ability. *P<0.05 *vs*. control group, #P<0.05 *vs*. IL-1β group. IL-1β: Interleukin-1β.

Apoptosis

It was uncovered by Annexin V-FITC/PI staining that IL-1β group had significantly more apoptotic cells relative to control group (P<0.05) and 12.5, 25 and 50 μg·mL^{-1} BAI groups (P<0.05) (Fig. 4). Taken together, BAI harbored a dose-dependent attenuation effect on the apoptosis of CESCs damaged by IL-1β.

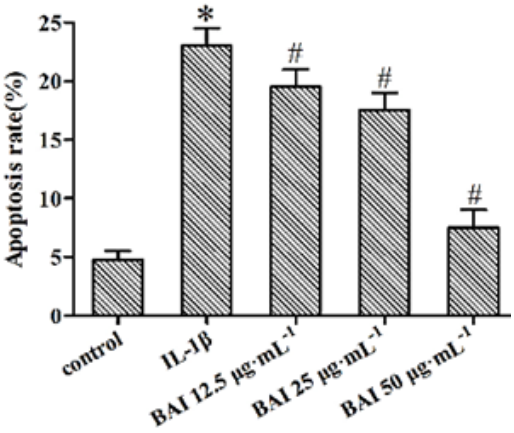

Fig. 4. Apoptosis ability. *P<0.05 *vs*. control group, #P<0.05 *vs*. IL-1β group. IL-1β: Interleukin-1β.

MRNA Expressions of IL-6, Acan and Type II and X Collagens

RT-qPCR results yielded that the IL-1â group had significantly increased mRNA expressions of IL-6 and type X collagen but decreased mRNA expressions of type II collagen and Acan relative to those in control group (P<0.05). The mRNA expressions of IL-6 and type X collagen were significantly lower, while those of type II collagen and Acan were higher in 12.5, 25 and 50 μg·mL^{-1} BAI groups than those in IL-1β group (P<0.05) (Fig. 5). Overall, BAI abated the levels of inflammatory factors in CESCs damaged by IL-1β and contributed to the dose-dependent relief of the loss of CESC matrix.

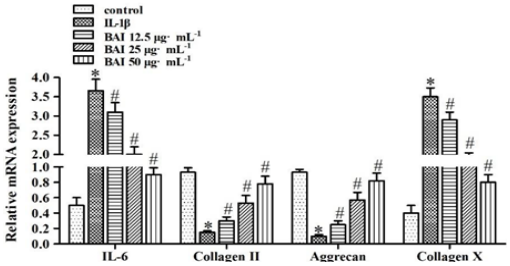

Fig. 5. MRNA expressions of IL-6, Acan and type II and X collagens. *P<0.05 *vs*. control group, #P<0.05 *vs*. IL-1β group. IL-1β: interleukin-1β; IL-6: interleukin-6; aggrecan: Acan

Protein Expressions of Type II collagen, Acan and MMP-3

It was observed from IF staining that IL-1β group displayed noticeably lower fluorescence intensities of type II collagen and a higher fluorescence intensity of MMP-3 than control group (P<0.05). Compared with IL-1β group, 12.5, 25 and 50 μg·mL^{-1} BAI groups had significantly higher fluorescence intensities of type II collagen and Acan but strikingly lower fluorescence intensity of MMP-3 (P<0.05) (Fig. 6). Thus, BAI decreased the level of MMPs in CESCs damaged by IL-1β and was advantageous to the dose-dependent alleviation of the loss of CESC matrix.

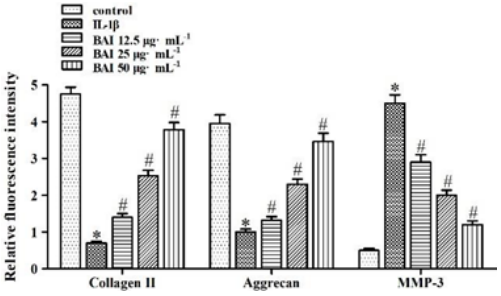

Fig. 6. Protein expressions of type II collagen, Acan and MMP-3. *P<0.05 *vs.* control group, #P<0.05 *vs.* IL-1β group. IL-1β: Interleukin-1β; Acan: aggrecan; MMP-3: matrix metalloproteinase-3

Protein Expressions of NF-κB p65, MMP-1 and MMP-13

The results of WB unveiled that IL-1β group displayed pronouncedly higher protein expressions of NF-κB p65, MMP-1 and MMP-13 than control group (P<0.05), which were noticeably lower in 12.5, 25 and 50 μg·mL^{-1} BAI groups than those in IL-1β group (P<0.05), suggesting that BAI reduces the expression of MMPs and exerts a dose-dependent inhibitory effect on the NF-κB pathway (Fig. 7).

Possible Mechanism of BAI in Inhibiting IL-1β-Stimulated Degradation of CESCs

BAI at different concentrations was advantageous to the proliferation but disadvantageous to the apoptosis of CESCs, reduced the levels of

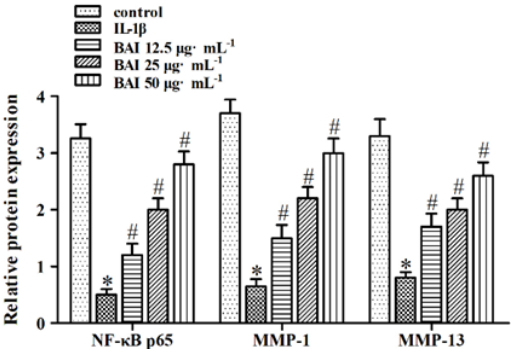

Fig. 7. Protein expressions of NF-κB p65, MMP-1 and MMP-13. *P<0.05 *vs.* control group, #P<0.05 *vs.* IL-1β group. IL-1β: Interleukin-1β; MMP: matrix metalloproteinase.

inflammatory factors IL-6 and MMP-1, MMP-3 and MMP-13, raised the levels of matrix components type II collagen and Acan, and relieved type X collagen-induced CEP calcification. Meanwhile, the protein expression of NF-κB p65 was also decreased by BAI dose-dependently. Therefore, we postulated that BAI, through regulating the NF-κB pathway, inhibited the apoptosis of CESCs and ECM degradation induced by IL-1β, and lowered the cellular inflammatory level, thereby alleviating the degradation of these cells (Fig. 8).

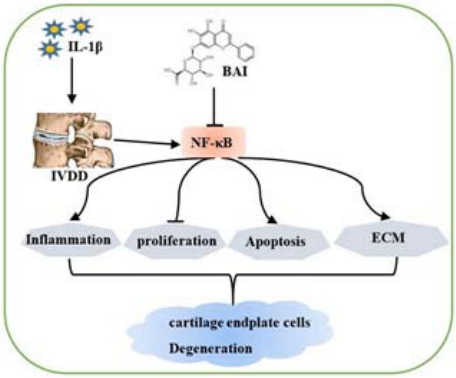

Fig. 8. Possible mechanism of BAI in inhibiting IL-1β-stimulated degradation of CESCs. BAI: Baicalin; IL-1β: interleukin-1β

DISCUSSION

IVDD refers to the aging and degeneration of the annulus fibrosus, nucleus pulposus and car-

tilage endplates (Eksi et al. 2022). The degeneration of IVD CEPs is the initiating factor of IVDD, closely related to apoptosis of cartilage endplates, inflammatory factors and matrix degradation (Ruiz Wills et al. 2018). It has been found that IL-1β has an abnormal expression in degenerated CESCs (Xiao et al. 2020). IL-1β can stimulate the NF-κB p65 signal transduction pathway, facilitate the synthesis of matrix-degrading enzymes and MMPs, and accelerate the apoptosis of CESCs and the degradation of ECM, thereby promoting IVDD (Zhang et al. 2018). Hence, it is of high value to explore drugs relieving CEP degeneration for mitigating IVDD.

Recently, the wide-range use of BAI has been observed in the clinical treatment of inflammatory diseases. For example, Zou et al. (2021) found that BAI alleviated *Mycoplasma gallisepticum*-induced pulmonary inflammation in chicken through inhibiting NF-κB p65 nuclear translocation. Chen et al. (2017) established an arthritis model through stimulating human chondrocytes by IL-1β, and found that BAI suppressed the activation of NF-κB, as well as the expressions of MMP-3 and MMP-13 and the degradation of type II collagen and Acan, thereby alleviating joint inflammation. In the present study, CESCs were stimulated by BAI and IL-1β. The results showed that 50 $\mu g \cdot mL^{-1}$ BAI had no toxic effect on CESCs, and attenuated IL-1β-induced apoptosis, restored cell proliferation ability, inhibited inflammation and kept the cell matrix structure, suggesting that BAI effectively relieves the degeneration of IVD CESCs.

IL-1β leads to metabolic imbalance in the ECM of CEPs (De Luca et al. 2020). The CESC matrix is primarily composed of type II collagen and Acan, the former of which not only regulates cartilage gene expression, but also increases ECM, and the latter can bind to hyaluronic acid to reduce joint wear and tear (Huang et al. 2021). In the case of degeneration and calcification of CESCs, the expressions of type II collagen and Acan drop down, thus affecting cell function. Moreover, type X collagen has an increased expression in degenerated chondrocytes, indicating chondrocyte hypertrophy (Singh et al. 2019). As a result, the influx of calcium ions into the matrix is further stimulated, and the calcification of CEPs is enhanced, further aggravating IVDD.

IL-1β can promote the production of MMPs that are primarily implicated in cell matrix metabolism (Chen et al. 2021). After normal CESCs are induced by IL-1β, the expressions of MMP-1, MMP-3 and MMP-13 are elevated. MMP-13 is more effective than other MMPs in the cleavage and degradation of type II collagen, so suppressing MMP-13 is able to efficiently prevent the degradation and loss of chondrocyte matrix (Hu and Ecker 2021). For example, Lakstins et al. (2021) found that the levels of type II collagen and Acan dropped down, fibrous collagen accumulated in hypertrophic chondrocytes, and CESCs displayed a degenerative phenotype in response to hypertrophy *in vitro*. Neidlinge et al. (2014) found that the expressions of IL-1β and MMP-3 declined in degenerated CEPs, being related to the severity of degeneration. In this study, the expressions of type II collagen, Acan, MMP-1, MMP-3 and MMP-13 were up-regulated, while that of type X collagen was down-regulated in 12.5, 25 and 50 $\mu g \cdot mL^{-1}$ BAI groups compared with those in IL-1β group. Taken together, BAI suppressed the expression of MMPs and the degradation of ECM, thereby alleviating the calcification of cartilage endplates.

IL-1β can activate NF-κB nuclear translocation and raise the expressions of other related pro-inflammatory factors (Cheleschi et al. 2018). NF-êB is a vital player in inflammation, which can increase the release of pro-inflammatory factors such as IL-6 and tumor necrosis factor-β. IL-6 is also the main inflammatory factor causing pain in patients with lumbar disc herniation, which is highly expressed in IVD tissue culture medium and CESCs (Hiyama et al. 2022). IL-1β also increases the level of IL-6, further activating macrophages, neutrophils and mastocytes, and amplifying the inflammatory cascade. For example, Luo et al. (2017) found that tripterine inhibited the protein expression of NF-κB p65 and the mRNA expression of IL-6, and effectively suppressed IL-1β-mediated degeneration of cartilage endplate cells. Zhao et al. (2019) found that pilose antler polypeptides abated the mRNA level of IL-6, further inhibiting inflammatory response. In this study, the expressions of NF-κB p65 and IL-6 were down-regulated in 12.5, 25 and 50 $\mu g \cdot mL^{-1}$ BAI groups compared with those in IL-1β group, suggesting that BAI inhibits the inflammatory cascade possibly through regulating the NF-κB signaling pathway.

CONCLUSION

To sum up, BAI inhibits the apoptosis of CESCs and the degradation of ECM induced by IL-1β, and reduces the cellular inflammatory level through regulating the NF-κB pathway, thereby alleviating the degradation of CESCs.

RECOMMENDATIONS

The findings herein provide new ideas for the prevention and treatment of IVDD.

ACKNOWLEDGMENT

This study was financially supported by Fund No. 2017D01C262.

DECLARATION OF CONFLICTING INTERESTS

The author(s) declared no potential conflicts of interest with respect to the research, authorship, and/or publication of this paper.

FUNDING

The author(s) received no financial support for the research, authorship, and/or publication of this paper.

REFERENCES

Cazzanelli P, Wuertz-Kozak K 2020. MicroRNAs in intervertebral disc degeneration, apoptosis, inflammation, and mechanobiology. *Int J Mol Sci*, 21: 3601.

Cheleschi S, Fioravanti A, De Palma A et al. 2018. Methylsulfonylmethane and mobilee prevent negative effect of IL-1β in human chondrocyte cultures via NF-κB signaling pathway. *Int Immunopharmacol*, 65: 129-139.

Chen C, Zhang C, Cai L et al. 2017. Baicalin suppresses IL-1β-induced expression of inflammatory cytokines via blocking NF-κB in human osteoarthritis chondrocytes and shows protective effect in mice osteoarthritis models. *Int Immunopharmacol*, 52: 218-226.

Chen HW, Zhang GZ, Liu MQ et al. 2021. Natural products of pharmacology and mechanisms in nucleus pulposus cells and intervertebral disc degeneration. *Evid Based Complement Altern Med*, 2021: 9963677.

De Luca P, de Girolamo L, Kouroupis D et al. 2020. Intervertebral disc and endplate cells response to IL-1β inflammatory cell priming and identification of molecular targets of tissue degeneration. *Eur Cells Mater*, 39: 227-248.

Eksi MS, Orhun Ö, Yasar AH et al. 2022. At what speed does spinal degeneration gear up? Aging paradigm in patients with low back pain. *Clin Neurol Neurosurg*, 215: 107187.

Hu Q, Ecker M 2021. Overview of MMP-13 as a promising target for the treatment of osteoarthritis. *Int J Mol Sci*, 22: 1742.

Huang B, Liu J, Wei X et al. 2021. Damage to the human lumbar cartilage endplate and its clinical implications. *J Anat*, 238: 338-348.

Huang T, Liu Y, Zhang C 2019. Pharmacokinetics and bioavailability enhancement of baicalin: A Review. *Eur J Drug Metab Pharmacokinet*, 44: 159-168.

Lakstins K, Yeater T, Arnold L, et al. 2021. Investigating the role of culture conditions on hypertrophic differentiation in human cartilage endplate cells. *J Orthop Res*, 39: 1204-1216.

Li J, Lin X, Liu X et al. 2020. Baicalin regulates Treg/Th17 cell imbalance by inhibiting autophagy in allergic rhinitis. *Mol Immunol*, 125: 162-171.

Li Y, Liu TT, Li YT, et al. 2020. Baicalin ameliorates cognitive impairment and protects microglia from LPS-induced neuroinflammation via the SIRT1/HMGB1 Pathway. *Oxid Med Cell Longev*, 2020: 4751349.

Liu ZM, Lu CC, Shen PC et al. 2021. Suramin attenuates intervertebral disc degeneration by inhibiting NF-κB signalling pathway. *Bone Joint Res*, 10: 498-513.

Luo D, Guo Y, Cheng Y et al. 2017. Natural product celastrol suppressed macrophage M1 polarization against inflammation in diet-induced obese mice via regulating Nrf2/HO-1, MAP kinase and NF-κB pathways. *Aging (Albany NY)*, 9: 2069-2082.

Luo L, Jian X, Sun H et al. 2021. Cartilage endplate stem cells inhibit intervertebral disc degeneration by releasing exosomes to nucleus pulposus cells to activate Akt/autophagy. *Stem Cells*, 39: 467-481.

Neidlinger-Wilke C, Boldt A, Brochhausen C et al. 2014. Molecular interactions between human cartilaginous endplates and nucleus pulposus cells: A preliminary investigation. *Spine*, 39: 1355-1364.

Ruiz Wills C, Foata B, Gonzalez Ballester MA et al. 2018. Theoretical explorations generate new hypotheses about the role of the cartilage endplate in early intervertebral disk degeneration. *Front Physiol*, 9: 1210.

Singh P, Marcu KB, Goldring MB et al. 2019. Phenotypic instability of chondrocytes in osteoarthritis: On a path to hypertrophy. *Ann New York Acad Sci*, 1442: 17-34.

Wang PZ, Liu J, Zhang SH et al. 2021. Baicalin promotes chondrocyte viability and the synthesis of extracellular matrix through TGF-â/Smad3 pathway in chondrocytes. *Am J Transl Res*, 13: 10908-10921.

Wang Y, Dai G, Wang L, et al. 2019. Identification of key genes potentially related to intervertebral disk degeneration by microarray analysis. *Genet Test Mol Biomark*, 23: 610-617.

Xiao L, Zhao Q, Hu B et al. 2020. METTL3 promotes IL-1β-induced degeneration of endplate chondrocytes by driving m6A-dependent maturation of miR-126-5p. *J Cell Mol Med*, 24: 14013-14025.

Yang S, Zhang F, Ma J et al. 2020. Intervertebral disc ageing and degeneration: The antiapoptotic effect of oestrogen. *Ageing Res Rev*, 57: 100978.

Zhang H, Li X, Wang J et al. 2021. Baicalin relieves Mycoplasma pneumoniae infection induced lung injury through

regulating microRNA 221 to inhibit the TLR4/NF κB signaling pathway. *Mol Med Rep,* 24: 571.

Zhang HJ, Liao HY, Bai DY et al. 2021. MAPK/ERK signaling pathway: A potential target for the treatment of intervertebral disc degeneration. *Biomed Pharmacother,* 143: 112170.

Zhang JF, Wang GL, Zhou ZJ et al. 2018. Expression of matrix metalloproteinases, tissue inhibitors of metalloproteinases, and interleukins in vertebral cartilage endplate. *Orthop Surg,* 10: 306-311.

Zhao S, Zuo W, Chen H et al. 2019. Effects of pilose antler peptide on bleomycin-induced pulmonary fibrosis in mice. *Biomed Pharmacother,* 109: 2078-2083.

Zou M, Yang L, Niu L et al. 2021. Baicalin ameliorates Mycoplasma gallisepticum-induced lung inflammation in chicken by inhibiting TLR6-mediated NF-κB signalling. *Br Poult Sci,* 62: 199-210.

Paper received for publication in January, 2022
Paper accepted for publication in March, 2022